Available online at www.sciencedirect.com

SciVerse ScienceDirect

Procedia - Social and Behavioral Sciences 54 (2012) 302 – 311

Procedia
Social and Behavioral Sciences

EWGT 2012

15th meeting of the EURO Working Group on Transportation

A general phase transition model for traffic flow on networks

Sébastien Blandin[a,*], Paola Goatin[b], Benedetto Piccoli[c], Alexandre Bayen[d], Daniel Work[e]

[a]*Research Scientist, IBM Singapore Research Collaboratory*
[b]*Research Scientist, INRIA Sophia Antipolis - Méditerranée*
[c]*Professor, Department of Mathematical Sciences, Rutgers University, Camden*
[d]*Associate Professor, Department of Electrical Engineering and Computer Sciences, Department of Civil and Environmental Engineering, University of California, Berkeley*
[e]*Assistant Professor, Department of Civil and Environmental Engineering, University of Illinois at Urbana-Champaign*

Abstract

A general class of macroscopic traffic flow models describing traffic dynamics on transportation networks is presented, with emphasis on the formulation of the junction problem. The type of admissible waves generated at junctions under the formulation proposed and their impact on vehicle energy consumption are described.

Keywords: hyperbolic conservation law; phase transition; network model; Riemman problem; macroscopic pollution model

1. Introduction

Macroscopic traffic models date back to the 1950s with the seminal work of Lighthill and Whitham (1956) and Richards (1956), who introduced one of the first scalar macroscopic traffic models. Later on, non-scalar models were introduced, to account for the existence of more complex phenomena (Papageorgiou et al., 1990; Aw and Rascle, 2000; Zhang, 2002; Colombo, 2003; Blandin et al., 2011b). In the general framework of hyperbolic conservation laws, these link models were extended to the case of net- works in Garavello and Piccoli (2006), see also Coclite et al. (2005); Colombo et al. (2010). For energy efficiency applications and traffic consumption and pollution optimization, the ability of models to accurately reproduce traffic patterns inducing spatio-temporal speed variations, and in particular higher-order traffic phenomena such as stop-and- go waves, hysteresis patterns, as well as the emergence of waves at junctions, is of critical interest. In this article, we extend state-of-art techniques for link and network macroscopic traffic modeling, and we propose an integrated formulation for modeling traffic energy consumption at a macroscopic level. The contributions of this article are the following:

* Corresponding author.
E-mail address: sblandin@sg.ibm.com

 doi:10.1016/j.sbspro.2012.09.749

- **Junction model for general phase transition model in the case of a Greenshields flux function**: the Riemann problem at the junction is formulated and a Riemann solver is constructed.
- **Design of numerical scheme for network phase transition model**: the modified Godunov scheme appropriate for the link version of the model is extended to the case of a network.
- **Analysis of a macroscopic consumption model**: a link-level power consumption model is considered and shown to provide good results on test network Riemann problems solution.

The rest of the article is organized as follows. Section 2 presents the phase transition model in the case of a Greenshield flux in congestion. A Riemann solver is described in details as well as a corresponding numerical scheme, the modified Godunov scheme. Section 3 is focused on a formulation of a junction model for the phase transition model. One of the main theoretical contributions of this work is the proof that under this formulation for the junction model, the phase transition model on networks is well-posed. In Section 4, a functional for traffic energy consumption modeling is considered for the solution to the phase transition model. Section 5 consists of numerical results based on the extension to the modified Godunov scheme, for a test Riemann problem at junction. Conclusive remarks and extensions to this work are discussed in section 6.

2. General phase transition model with Greenshields flux function: link formulation

The phase transition model of macroscopic traffic flow (Colombo, 2003) proposes to consider different systems of conservation laws to model different phases traffic flow. It was shown in Blandin et al. (2011b) that the phase transition model could be generalized to an arbitrary flux function in the congested phase, and considered in this phase as an extension to classical scalar macroscopic traffic models that accounts for heterogeneous driving behaviors, see Blandin et al. (2011a) for an extensive description of model capabilities and numerical validation. In this section we describe the instantiation of the general phase transition model used in this article, using a *Greenshields* flux function (Greenshields, 1935) in congestion.

2.1. Model dynamics on a link

We model traffic phenomena as constituted of two phases, the *free-flow* phase Ω_f and the *congestion* phase Ω_c. In free-flow, the traffic state is represented by the density of vehicle ρ. In congestion, the traffic state is represented by the couple $u \doteq (\rho, p)$, where p denotes a perturbation. The system evolves according to a system of conservation laws:

$$\begin{cases} \partial_t \rho + \partial_x(\rho v) = 0 & \text{for } \rho \in \Omega_f \\ \begin{cases} \partial_t \rho + \partial_x(\rho v) = 0 \\ \partial_t p + \partial_x(p v) = 0 \end{cases} & \text{for } (\rho, p) \in \Omega_c, \end{cases} \tag{1}$$

where v denotes the speed of vehicles, defined as:

$$v = \begin{cases} v_f(\rho) := V & \text{for } \rho \in \Omega_f \\ v_c(\rho, p) := \left(1 - \frac{\rho_{\max}}{\rho}\right)\left(a(\rho - \rho_c) + \frac{\rho_c V}{\rho_c - \rho_{\max}}\right)(1 + p) & \text{for } (\rho, p) \in \Omega_c. \end{cases} \tag{2}$$

In (2) V denotes the free-flow speed, ρ_c, $\rho_{\max}$ respectively denote the critical, maximal density, and the parameter a belongs to the interval $\left[-\frac{\rho_c V}{(\rho_c - \rho_{\max})^2}, 0\right[$, in order to have a concave decreasing flux function in $(\rho, \rho v)$ coordinates, for the congested phase, in the case where $p = 0$. The domains Ω_f, Ω_c denoting the free-flow, congestion phase respectively, are defined as follows:

$$\begin{cases} \Omega_f = \{(\rho, p) \mid (\rho, p) \in [0, \rho_{\max}] \times [p_-, p_+] \ , \ v_c(\rho, p) = V \ , \ 0 \le \rho \le \rho_{c+}\} \\ \Omega_c = \left\{(\rho, p) \mid (\rho, p) \in [0, \rho_{\max}] \times [p_-, p_+] \ , \ v_c(\rho, p) < V \ , \ \frac{p_-}{\rho_{\max}} \le \frac{p}{\rho} \le \frac{p_+}{\rho_{\max}}\right\} \end{cases} \tag{3}$$

where p_-, p_+ denote the bounds on the perturbation, and ρ_{c+} is defined by $v_c(\rho_{c+}, \rho_{c+} p_+ / \rho_{\max}) = V$.

We further impose $q_- > -\frac{a \rho_{\max}}{\frac{\rho_c V}{\rho_c - \rho_{\max}} + a(2\rho_{\max} - \rho_c)}$ to guarantee that, in the congested set Ω_c, the 1-Lax curves of the system are concave in $(\rho, \rho v)$ coordinates.

2.2. Riemann solver on a link

The Riemann problem for the system (1) is a Cauchy problem with piecewise constant initial condition:

$$u(0,x) = \begin{cases} u_l & \text{if} \quad x < 0 \\ u_r & \text{if} \quad x > 0 \end{cases} \tag{4}$$

In the following we note u_m and $u_{m\_}$ respectively the solutions to systems:

$$\begin{cases} \frac{p_l}{\rho_l} = \frac{p_m}{\rho_m}, \\ v_c(\rho_r, p_r) = v_c(\rho_m, p_m), \end{cases} \qquad \begin{cases} \frac{p_-}{\rho_{\max}} = \frac{p_{m\_}}{\rho_{m\_}}, \\ v_c(\rho_r, p_r) = v_c(\rho_{m\_}, p_{m\_}). \end{cases}$$

The Riemann solver defined in Blandin et al. (2011b) reads:

- **Case 1**: $u_l \in \Omega_f$ and $u_r \in \Omega_f$. The solution consists of a contact discontinuity from u_l to u_r.
- **Case 2**: $u_l \in \Omega_c$ and $u_r \in \Omega_c$. The solution consists of a 1-shock wave or 1-rarefaction wave from u_l to u_m and a 2-contact discontinuity from u_m to u_r.
- **Case 3**: $u_l \in \Omega_c$ and $u_r \in \Omega_f$. The solution consists of a 1-rarefaction wave from u_l to u_m and a contact discontinuity from u_m to u_r.
- **Case 4**: $u_l \in \Omega_f$ and $u_r \in \Omega_c$. The solution consists of a shock-like phase transition from u_l to $u_{m\_}$ and of a 2-contact discontinuity from u_p to u_r.

2.3. Modified Godunov scheme on a link

The modified Godunov scheme introduced in Chalons and Goatin (2008) is an extension to the classical Godunov scheme (Godunov, 1959), appropriate for the non-convex state-space $\Omega_f \cup \Omega_c$. The derivation of the modified Godunov scheme is as follows:

- Resolution of Riemann problems defined by the datum of neighboring cells on the same link.
- Identification of the neighboring cells for which the solution to the Riemann problem includes a phase transition.
- Averaging of the solutions on spatial domains for which the solution belongs to a unique phase.
- Sampling and projection of the computed solution onto the regular mesh.

We refer the interested reader to Chalons and Goatin (2008) and Blandin et al. (2011b) for more details on the modified Godunov scheme. The extension of the modified Godunov scheme to the junction problem for the phase transition model, which is the focus of this article, is described in Section 3.2.

3. General phase transition model with Greenshields flux function: junction formulation

In this section we present the formulation of the junction problem for the phase transition model detailed in the previous section, following Colombo et al. (2010).

3.1. The Riemann problem at junction

For notational convenience, we introduce the following short form

$$\partial_t \mathbf{u} + \partial_x \mathbf{f}(\mathbf{u}) = 0 \tag{5}$$

for the phase transition model (1), where

$$\begin{cases} \mathbf{u} = (\rho, p) \quad \text{and} \quad \mathbf{f}(\mathbf{u}) = (\rho V, p V) , & \text{if} \quad (\rho, p) \in \Omega_f , \\ \mathbf{u} = (\rho, p) \quad \text{and} \quad \mathbf{f}(\mathbf{u}) = (\rho v_c(\rho, p), p\, v_c(\rho, p)) , & \text{if} \quad (\rho, p) \in \Omega_c . \end{cases}$$

Following Garavello and Piccoli (2006), Definition 4.1.1, by road network we mean a couple $(\mathcal{I}, \mathcal{J})$, where $\mathcal{I}$ is a finite collection of unidirectional roads and $\mathcal{J}$ is a set of junctions. Each road is modelled by real intervals $I_i =]a_i, b_i[$,

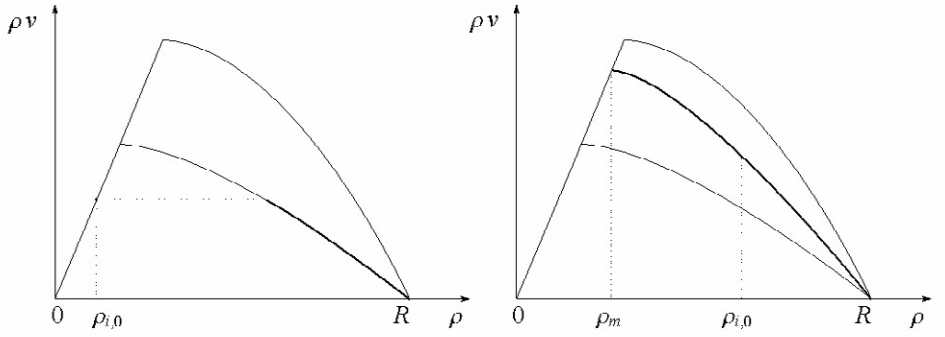

Figure 1. Notations used in the definition of the sets $O_i(\mathbf{u}_{i,0})$, $i = 1, \ldots, n$. Left: $\mathbf{u}_{i,0} \in \Omega_f$. Right: $\mathbf{u}_{i,0} \in \Omega_c$.

$i = 1, \ldots, M$, while each J consists of two sets $Inc(J) \subset \{1, \ldots, M\}$ and $Out(J) \subset \{1, \ldots, M\}$ corresponding to incoming and outgoing roads of J.

Fix a junction J and assume for simplicity that $Inc(J) = \{1, \ldots, n\}$ and $Out(J) = \{n+1, \ldots, n+m\}$. A Riemann problem at J is a Cauchy problem with initial data constant on each incoming and outgoing road:

$$\begin{cases} \partial_t \mathbf{u}_i + \partial_x f(\mathbf{u}_i) = 0, \\ \mathbf{u}_i(0,x) = \mathbf{u}_{i,0} \end{cases} \qquad i = 1, \ldots, n+m. \tag{6}$$

To construct an admissible solution we require the following properties:

(J1) it consists of waves with negative speed in incoming roads;
(J2) it consists of waves with positive speed in outgoing roads;
(J3) it conserves the number of cars at J.

3.1.1. Incoming roads: attainable values at the junction

To satisfy condition **(J1)**, only waves with negative speed can be produced on incoming roads. Thus, we determine all states which can be connected to an initial state (to the right) by waves with negative speed. In particular, we determine the maximum flux $\gamma_i^{\max}$ that can be reached from an initial datum $\mathbf{u}_{i,0} = (\rho_{i,0}, p_{i,0})$ by means of waves with negative speed only.

We start describing the sets of fluxes corresponding to states that can be connected to $\mathbf{u}_{i,0}$ on the right using non positive waves only. Let $\mathbf{u}_m = (\rho_m, p_m)$ be the point in Ω_c defined by

$$\begin{cases} \dfrac{p_m}{\rho_m} = \dfrac{p_{i,0}}{\rho_{i,0}}, \\ v_c(\mathbf{u}_m) = V, \end{cases}$$

see Figure 1, right. The sets of reachable fluxes are then given by

$$O_i(\mathbf{u}_{i,0}) = \begin{cases} [0, \rho_{i,0} V] & \text{if } \mathbf{u}_{i,0} \in \Omega_f, \\ [0, \rho_m V] & \text{if } \mathbf{u}_{i,0} \in \Omega_c, \end{cases}$$

for $i = 1, \ldots, n$. The corresponding maximum fluxes are given by:

$$\gamma_i^{\max}(\mathbf{u}_{i,0}) = \begin{cases} \rho_{i,0} V & \text{if } \mathbf{u}_{i,0} \in \Omega_f, \\ \rho_m V & \text{if } \mathbf{u}_{i,0} \in \Omega_c. \end{cases} \tag{7}$$

Proposition 3.1. *Given an initial datum $\mathbf{u}_{i,0}$ on an incoming road and $\hat{\gamma} \in O_i$, there exists a unique $\hat{\mathbf{u}}_i \in \Omega$ such that the Riemann problem $(\mathbf{u}_{i,0}, \hat{\mathbf{u}}_i)$ is solved by waves with negative speed and $\mathbf{f}_1(\hat{\mathbf{u}}_i) = \hat{\gamma}$.*

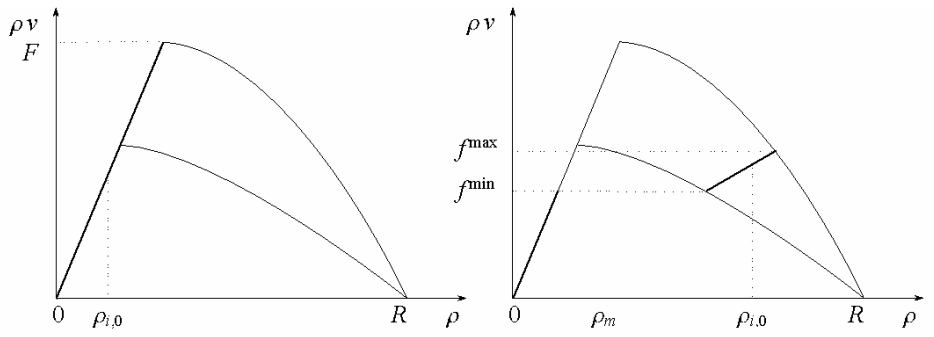

Figure 2. Notations used in the definition of the sets $O_j(\mathbf{u}_{j,0})$, $j = n+1,\dots,n+m$. Left: $\mathbf{u}_{j,0} \in \Omega_f$. Right: $\mathbf{u}_{j,0} \in \Omega_c$.

Notice that $\hat{\mathbf{u}}_i \in \Omega_f$ iff $\hat{\gamma} = \gamma_i^{\max}(\mathbf{u}_{i,0})$, otherwise $\hat{\mathbf{u}}_i \in \Omega_c$ (see Figure 1).

3.1.2. Outgoing roads: maximal flux at the junction

To satisfy condition **(J2)**, only waves with positive speed can be produced on outgoing roads. Thus we determine all states, and the corresponding set of fluxes, which can be connected to an initial state $\mathbf{u}_{j,0}$ (to the left) using waves with positive speed. We introduce the fluxes F and $f^{\max}$ defined as follows (see Figure 2):

- $F = \rho_{c+} V = \rho_{c+} v_c(\rho_{c+}, p_+)$ is the maximal flux supported by the road;
- for $\mathbf{u}_{j,0} \in \Omega_c$, $f^{\max} = f^{\max}(\mathbf{u}_{j,0}) = \rho^{\max} v_c(\rho^{\max}, p^{\max})$, where $\mathbf{u}^{\max} = (\rho^{\max}, p^{\max})$ is the solution in Ω_c of the system

$$\begin{cases} \dfrac{p^{\max}}{\rho^{\max}} = \dfrac{p_+}{R}, \\ v_c(\mathbf{u}^{\max}) = v_c(\mathbf{u}_{j,0}). \end{cases}$$

The sets of reachable fluxes are given by

$$O_j(\mathbf{u}_{j,0}) = \begin{cases} [0, F] & \text{if } \mathbf{u}_{j,0} \in \Omega_f, \\ [0, f^{\max}(\mathbf{u}_{j,0})] & \text{if } \mathbf{u}_{j,0} \in \Omega_c, \end{cases}$$

for $j = n+1,\dots,n+m$. Since the sets O_j are convex, the corresponding maximum fluxes are defined accordingly:

$$\gamma_j^{\max}(\mathbf{u}_{j,0}) = \begin{cases} F & \text{if } \mathbf{u}_{j,0} \in \Omega_f, \\ f^{\max}(\mathbf{u}_{j,0}) & \text{if } \mathbf{u}_{j,0} \in \Omega_c. \end{cases} \tag{8}$$

Proposition 3.2. *Given an initial datum $\mathbf{u}_{j,0}$ on an outgoing road and $\hat{\gamma} \in O_j$, there exists a unique $\hat{\mathbf{u}}_j \in \Omega$ such that the Riemann problem $(\hat{\mathbf{u}}_j, \mathbf{u}_{j,0})$ is solved by waves with positive speed and $\mathbf{f}_1(\hat{\mathbf{u}}_j) = \hat{\gamma}$.*

Notice that $\hat{\mathbf{u}}_i \in \Omega_f$ except if $\mathbf{u}_{j,0} \in \Omega_c$ and $\hat{\mathbf{u}}_i \in [f^{\min}(\mathbf{u}_{j,0}), f^{\max}(\mathbf{u}_{j,0})]$, where $f^{\min} = f^{\min}(\mathbf{u}_{j,0}) = \rho^{\min} v_c(\rho^{\min}, p^{\min})$, where $\mathbf{u}^{\min} = (\rho^{\min}, p^{\min})$ is the solution in Ω_c of the system

$$\begin{cases} \dfrac{p^{\min}}{\rho^{\min}} = \dfrac{p_-}{R}, \\ v_c(\mathbf{u}^{\min}) = v_c(\mathbf{u}_{j,0}). \end{cases}$$

3.1.3. The Riemann Solver at the junction

We construct a solution to (6) following the procedure introduced in Coclite et al. (2005) for the LWR model. First of all we need to define a suitable set of distribution matrices. Consider the set

$$\mathcal{A} := \left\{ A = \{a_{ji}\}_{i=1,\dots,n,\ j=n+1,\dots,n+m} : 0 < a_{ji} < 1 \ \forall i,j, \ \sum_{j=n+1}^{n+m} a_{ji} = 1 \ \forall i \right\}. \tag{9}$$

Let $\{e_1, \dots, e_n\}$ be the canonical basis of $\mathbb{R}^n$. For every $i = 1, \dots, n$, we denote $H_i = \{e_i\}^\perp$. If $A \in \mathcal{A}$, then we write, for every $j = n+1, \dots, n+m$, $a_j = (a_{j1}, \dots, a_{jn}) \in \mathbb{R}^n$ and $H_j = \{a_j\}^\perp$. Let $\mathcal{K}$ be the set of indexes $\mathbf{k} = (k_1, \dots, k_\ell)$, $1 \le \ell \le n-1$, such that $0 \le k_1 < k_2 < \cdots < k_\ell \le n+m$ and for every $\mathbf{k} \in \mathcal{K}$ define

$$H_{\mathbf{k}} := \bigcap_{h=1}^{\ell} H_{k_h}.$$

Writing $\mathbf{1} = (1, \dots, 1) \in \mathbb{R}^n$ and following Coclite et al. (2005) we define the set

$$\mathfrak{N} := \left\{ A \in \mathcal{A} : \mathbf{1} \notin H_{\mathbf{k}}^{\perp} \text{ for every } \mathbf{k} \in \mathcal{K} \right\}. \tag{10}$$

Notice that, if $n > m$, then $\mathfrak{N} = \emptyset$. In this case one can recover uniqueness of the solution introducing "right-of-way" parameter as explained in Garavello and Piccoli (2009). The matrices of $\mathfrak{N}$ give rise to a unique solution to Riemann problems at J, constructed as follows:

1. Fix a matrix $A \in \mathfrak{N}$ and consider the closed, convex and not empty set
$$\Lambda = \left\{ (\gamma_1, \dots, \gamma_n) \in \prod_{i=1}^{n} [0, \gamma_i^{\max}] : A \cdot (\gamma_1, \dots, \gamma_n)^T \in \prod_{j=n+1}^{n+m} [0, \gamma_j^{\max}] \right\}. \tag{11}$$
2. Find the point $(\bar\gamma_1, \dots, \bar\gamma_n) \in \Lambda$ which maximizes the function
$$E(\gamma_1, \dots, \gamma_n) = \gamma_1 + \cdots + \gamma_n \tag{12}$$
and define $(\bar\gamma_{n+1}, \dots, \bar\gamma_{n+m})^T := A \cdot (\bar\gamma_1, \dots, \bar\gamma_n)^T$. Since $A \in \mathfrak{N}$, the point $(\bar\gamma_1, \dots, \bar\gamma_n)$ is uniquely defined.
3. For every $i \in \{1, \dots, n\}$, set $\hat{\mathbf{u}}_i$ either by $\mathbf{u}_{i,0}$ if $\mathbf{f}_1(\mathbf{u}_{i,0}) = \bar\gamma_i$, or by the solution to $\mathbf{f}_1(\mathbf{u}) = \bar\gamma_i$ given by Proposition 3.1. For every $j \in \{n+1, \dots, n+m\}$, set $\hat{\mathbf{u}}_j$ either by $\mathbf{u}_{j,0}$ if $\mathbf{f}_1(\mathbf{u}_{j,0}) = \bar\gamma_j$, or by the solution to $\mathbf{f}_1(\mathbf{u}) = \bar\gamma_j$ given by Proposition 3.2.

3.2. Numerical scheme at the junction

We introduce a space step Δx and a time step Δt, both assumed to be constant and satisfying the classical CFL condition. We discretize each road I_l, $l = 1, \dots, n+m$, involved in the junction with a mesh of size Δx: we set $x_{l,k} = (k - 1/2)\Delta x$ for $k = 1, \dots, N_l$, and $t^n = n\Delta t$ for $n \in \mathbb{N}$. Moreover we set $x_{l,k\pm1/2} = x_{l,k} \pm \Delta x/2$, and we define the cells $C_{l,k}^n = \{t^n\} \times [x_{l,k-1/2}, x_{l,k+1/2}[$, whose length is equal to Δx. In the following we will call $\mathbf{u}_{l,k}^n$ the (approximated value) of $\mathbf{u} = (\rho, p)$ at the point $(t^n, x_{l,k})$, and, by extension, in $C_{l,k}^n$.

We need to generalize the modified Godunov scheme introduced in Chalons and Goatin (2008) and described in Blandin et al. (2011b) to handle the coupling at the junction.

At each time step, first of all we compute the maximized fluxes $\bar\gamma_l^n = \bar\gamma_l(t^n)$, $l = 1, \dots, n+m$, and the corresponding conserved quantities $\hat{\mathbf{u}}_l^n$, by using the procedure described in the previous Section 3.1.3, where we have taken $\mathbf{u}_{i,0} = \mathbf{u}_{i,N_i}^n$ for $i = 1, \dots, n$, and $\mathbf{u}_{j,0} = \mathbf{u}_{j,1}^n$ for $j = n+1, \dots, n+m$.

Then, let $\nu_{J,l}^n$ denote the speed of the phase transition (if any) in the solution of the Riemann problem between $\mathbf{u}_{i,N_i}^n$ and $\hat{\mathbf{u}}_i^n$ for for $i = 1, \dots, n$ (respectively, between $\hat{\mathbf{u}}_j^n$ and $\mathbf{u}_{j,1}^n$ for $j = n+1, \dots, n+m$). By construction, $\nu_{J,l}^n \le 0$ for $l \le n$ and $\nu_{J,l}^n \ge 0$ for $l > n$. Setting $\bar x_{l,N_l+1/2}^{n+1} = x_{l,N_l+1/2}^{n+1} + \nu_{J,l}^n \Delta t$ for $l \le n$, respectively $\bar x_{l,1/2}^{n+1} = x_{l,1/2}^{n+1} + \nu_{J,l}^n \Delta t$ for $l > n$, we can define the modified cells

$$\bar C_{l,N_l}^{n+1} = \{t^{n+1}\} \times [\bar x_{l,N_l-1/2}^{n+1}, \bar x_{l,N_l+1/2}^{n+1}[\quad \text{for } l \le n,$$

which have length $\Delta \bar x_{l,N_l}^n = \bar x_{l,N_l+1/2}^{n+1} - \bar x_{l,N_l-1/2}^{n+1}$, respectively

$$\bar C_{l,1}^{n+1} = \{t^{n+1}\} \times [\bar x_{l,1/2}^{n+1}, \bar x_{l,3/2}^{n+1}[\quad \text{for } l > n,$$

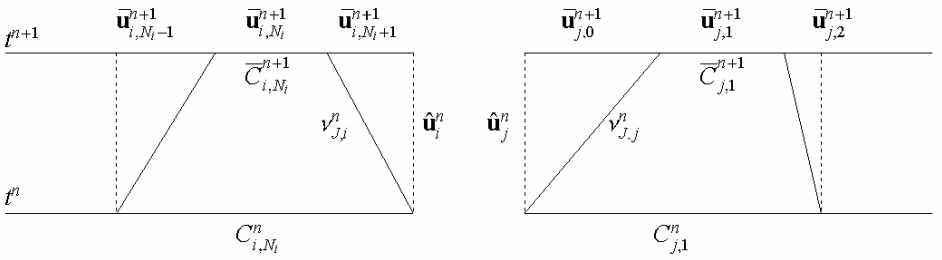

Figure 3. Notations used in the construction of the modified Godunov method at the junction. Left: incoming roads. Right: outgoing roads.

which have length $\Delta\bar{x}^n_{i,1} = \bar{x}^{n+1}_{i,3/2} - \bar{x}^{n+1}_{i,1/2}$. We can thus compute the averaging step on the modified cells as follows:

$$\begin{aligned}\Delta\bar{x}^{n+1}_{i,N_i}\ \bar{\mathbf{u}}^{n+1}_{i,N_i} &= \Delta x\ \mathbf{u}^n_{i,N_i} - \Delta t\left(g\left(\nu^{n,-}_{J,i}, \mathbf{u}^n_{i,N_i}, \hat{\mathbf{u}}^n_i\right) - \nu^n_{J,i}\ u_R\left(\nu^{n,-}_{J,i}, \mathbf{u}^n_{i,N_i}, \hat{\mathbf{u}}^n_i\right)\right)\\ &\quad + \Delta t\left(g\left(\nu^{n,+}_{i,N_i-1/2}, \mathbf{u}^n_{i,N_i-1}, \mathbf{u}^n_{i,N_i}\right) - \nu^n_{i,N_i-1/2}\ u_R\left(\nu^{n,+}_{i,N_i-1/2}, \mathbf{u}^n_{i,N_i-1}, \mathbf{u}^n_{i,N_i}\right)\right)\end{aligned}$$

for $i \le n$, and

$$\begin{aligned}\Delta\bar{x}^{n+1}_{i,1}\ \bar{\mathbf{u}}^{n+1}_{i,1} &= \Delta x\ \mathbf{u}^n_{i,1} - \Delta t\left(g\left(\nu^{n,-}_{i,3/2}, \mathbf{u}^n_{i,1}, \mathbf{u}^n_{i,2}\right) - \nu^n_{i,3/2}\ u_R\left(\nu^{n,-}_{i,3/2}, \mathbf{u}^n_{i,1}, \mathbf{u}^n_{i,2}\right)\right)\\ &\quad + \Delta t\left(g\left(\nu^{n,+}_{J,i}, \hat{\mathbf{u}}^n_i, \mathbf{u}^n_{i,1},\right) - \nu^n_{J,i}\ u_R\left(\nu^{n,+}_{J,i}, \hat{\mathbf{u}}^n_i, \mathbf{u}^n_{i,1},\right)\right)\end{aligned}$$

for $i > n$. Moreover, for all $i \le n$ (such that $\nu^n_{J,i} < 0$) we define $\bar{\mathbf{u}}^{n+1}_{i,N_i+1}$ by

$$(x_{i,N_i+1/2} - \bar{x}_{i,N_i+1/2})\,\bar{\mathbf{u}}^{n+1}_{i,N_i+1} = \Delta t\left(g\left(\nu^{n,+}_{J,i}, \mathbf{u}^n_{i,N_i}, \hat{\mathbf{u}}^n_i\right) - \nu^n_{J,i}\ u_R\left(\nu^{n,+}_{J,i}, \mathbf{u}^n_{i,N_i}, \hat{\mathbf{u}}^n_i\right) - \bar{\gamma}^n_i\right),$$

and for all $i > n$ (such that $\nu^n_{J,i} > 0$) we define $\bar{\mathbf{u}}^{n+1}_{i,0}$ by

$$(\bar{x}_{i,1/2} - x_{i,1/2})\,\bar{\mathbf{u}}^{n+1}_{i,0} = -\Delta t\left(g\left(\nu^{n,-}_{J,i}, \hat{\mathbf{u}}^n_i, \mathbf{u}^n_{i,1},\right) - \nu^n_{J,i}\ u_R\left(\nu^{n,-}_{J,i}, \hat{\mathbf{u}}^n_i, \mathbf{u}^n_{i,1},\right) - \bar{\gamma}^n_i\right).$$

Finally, we apply the usual sampling technique to recover the approximate values on the original cells $\bar{C}^{n+1}_{i,N_i}$, $i \le n$:

$$\mathbf{u}^{n+1}_{i,N_i} = \begin{cases} \bar{\mathbf{u}}^{n+1}_{i,N_i-1} & \text{if } a_n \in \left]0, \max\left(\frac{\Delta t}{\Delta\bar{x}^n_{i,N_i}}\,\nu^n_{i,N_i-1/2}, 0\right)\right] \\ \bar{\mathbf{u}}^{n+1}_{i,N_i} & \text{if } a_n \in \left]\max\left(\frac{\Delta t}{\Delta\bar{x}^n_{i,N_i}}\,\nu^n_{N_i-1/2}, 0\right), 1 + \min\left(\frac{\Delta t}{\Delta\bar{x}^n_{i,N_i}}\,\nu^n_{J,i}, 0\right)\right[\\ \bar{\mathbf{u}}^{n+1}_{i,N_i+1} & \text{if } a_n \in \left[1 + \min\left(\frac{\Delta t}{\Delta\bar{x}^n_{i,N_i}}\,\nu^n_{J,i}, 0\right), 1\right[, \end{cases} \tag{13}$$

respectively on $\bar{C}^{n+1}_{i,1}$, $i > n$, where

$$\mathbf{u}^{n+1}_{i,1} = \begin{cases} \bar{\mathbf{u}}^{n+1}_{i,0} & \text{if } a_n \in \left]0, \max\left(\frac{\Delta t}{\Delta\bar{x}^n_{i,1}}\,\nu^n_{J,i}, 0\right)\right] \\ \bar{\mathbf{u}}^{n+1}_{i,1} & \text{if } a_n \in \left]\max\left(\frac{\Delta t}{\Delta\bar{x}^n_{i,1}}\,\nu^n_{J,1}, 0\right), 1 + \min\left(\frac{\Delta t}{\Delta\bar{x}^n_{i,1}}\,\nu^n_{i,3/2}, 0\right)\right[\\ \bar{\mathbf{u}}^{n+1}_{i,2} & \text{if } a_n \in \left[1 + \min\left(\frac{\Delta t}{\Delta\bar{x}^n_{i,1}}\,\nu^n_{i,3/2}, 0\right), 1\right[. \end{cases} \tag{14}$$

4. Power consumption model

In this section we consider the modeling of traffic energy consumption from vehicles, using the solutions to the system of conservation laws (1) describing the phase transition model.

The power consumption associated with the dynamics of vehicles (Simpson, 2005) can be modeled as the sum of

the power losses due to aerodynamic and rolling drag, and the power spent on vehicle acceleration and hill-climbing:

$$\mathcal{P}\left(v, \frac{dv}{dt}\right) = \mathcal{P}_{aero} + \mathcal{P}_{roll} + \mathcal{P}_{acc} + \mathcal{P}_{hill} \tag{15}$$

$$= k_{aero}\, v^3 + k_{roll}\, v + k_{acc}\, v \frac{dv}{dt} + k_{hill}\, v \tag{16}$$

where $k_{aero} = 0.5\, d C_D A$ with d the air density, C_D the drag coefficient, A the frontal area of the vehicle, $k_{roll} = C_{RR}\, m\, g$ with C_{RR} the rolling coefficient, m the mass of the vehicle, g the gravitational acceleration, $k_{acc} = k_m\, m$ with k_m a factor due to rotational inertia of the power-train, and $k_{hill} = m\, g\, Z$ with Z the grade. In the following we consider the case of a flat road without wind, hence the last term in equation (15) disappears and the speed corresponds to the vehicle speed. We compute the average power for a stretch of road $[a, b]$ at time t as follows

$$\mathcal{P}_{link}(t) = \frac{1}{b-a} \int_a^b \mathcal{P}\left(v(t,x), \frac{dv}{dt}(t,x)\right) \rho(t,x)\, dx \tag{17}$$

which can be computed from $v(\cdot,\cdot)$ given by the solution of the phase transition model, and using the equality

$$\frac{dv}{dt} = \frac{\partial v}{\partial t} + v \frac{\partial v}{\partial x}.$$

Since the phase transition model implicitly models infinite acceleration (existence of shock waves), in the following section, we illustrate the power consumption results on the first two components of the power consumption.

5. Numerical results

In this section we present the modeling abilities of the network phase transition model on a Riemann problem.

5.1. Experiment setting

We consider the case of a junction with 2 incoming links and 1 outgoing link, of 1 mile each. The fundamental diagram parameters are as follows:

- Link 1 (incoming): $V = 90$ mph, $R = 600$ vpm, $\sigma = 120$ vpm, $\sigma_- = 114$ vpm, $\sigma_+ = 138$ vpm.
- Link 2 (incoming): $V = 30$ mph, $R = 200$ vpm, $\sigma = 40$ vpm, $\sigma_- = 38$ vpm, $\sigma_+ = 46$ vpm.
- Link 3 (outgoing): $V = 60$ mph, $R = 400$ vpm, $\sigma = 80$ vpm, $\sigma_- = 76$ vpm, $\sigma_+ = 92$ vpm.

For physical considerations, in the remainder of the article, we represent the state in density-velocity coordinates, where the velocity is computed from the state variables (ρ, p) using the expression of the velocity function (2).

We consider the following Riemann datum for the junction:

$$(\rho_i, v_i)(t=0,x) = \begin{cases} (280, 29) & \text{if} \quad i = 1 \\ (93, 10) & \text{if} \quad i = 2 \\ (187, 19) & \text{if} \quad i = 3 \end{cases} \tag{18}$$

with the units being vehicles per mile (vpm) for density and miles per hour (mph) for speed.

5.2. Numerical solution to network phase transition model

The value of the solution to the Riemann problem (18) at the junction, computed according to the numerical scheme defined in Section 3.2, with 100 space cells for each link, is represented at time $T = 2$ minutes in Figure 4.

The waves composing the solution to the Riemann problem (18) at the junction, according to the Riemann solver introduced in Section 3.1, have the following traffic interpretation.

According to the initial datum defined in (18), the sum of the incoming flows equals 9050 vph which is greater than the maximal allowable flow on the outgoing link, computed as equal to 4201 vph according to equation (8) second

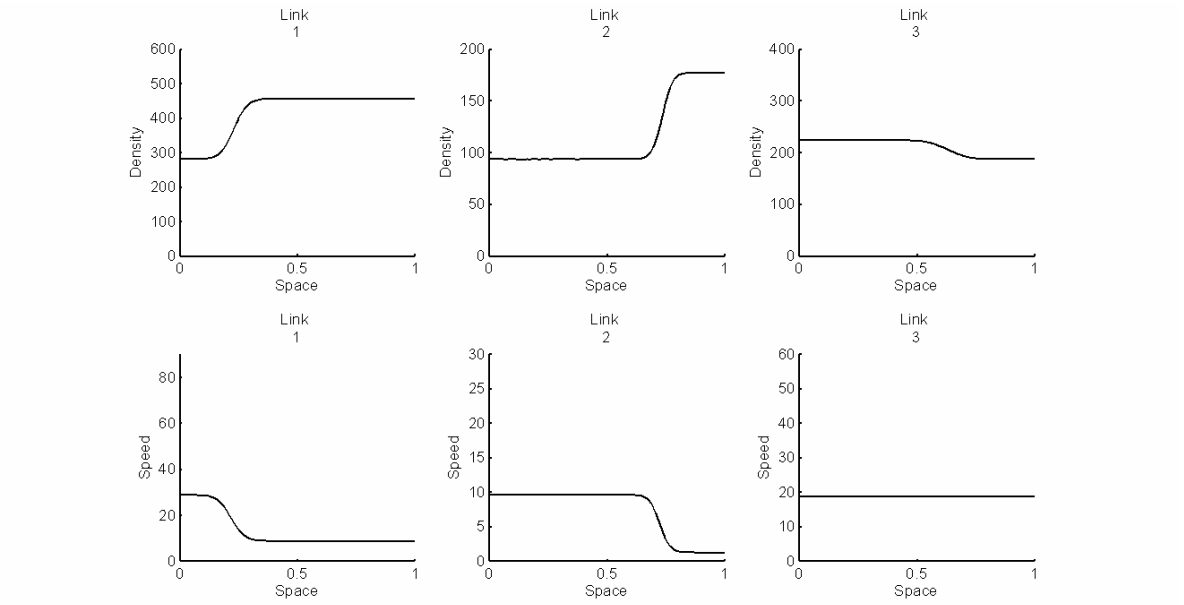

Figure 4. Solution to the Riemann problem at junction at time $T = 2$ minutes, represented in density (top row) and speed (bottom row) coordinates. A 1-shock wave emerging from the junction is visible for the incoming links (left and middle columns), whereas a 2-contact discontinuity propagates on the outgoing link (right column).

case, and its illustration on Figure 2, right. In other words, in this case, the traffic supply downstream of the junction is lower than the traffic demand upstream of the junction. The maximal flow through the junction is thus defined from the supply side as the maximal allowable flow on the outgoing link 4201 vph, which, given the assignment matrix $A = (1, 1)$ for the case of 2 incoming links and 1 outgoing link, induces the respective junction flows 3981 vph and 220 vph on incoming links 1, 2 respectively.

The state arising at the end points on the incoming links due to the flow constraint at the junction can be computed using the well-posedness constraints detailed in Section 3.1.1 for the incoming links, and illustrated for the case of congestion in Figure 1, right. In this case, a state with density $\rho = 455$ vpm, speed $v = 8.5$ mph arises at the downstream end of link 1, and a state with density $\rho = 177$ vpm, speed $v = 1.9$ mph, arises at the downstream end of link 2. On these two links, a 1-shock wave propagating backward is created.

On the outgoing link, the interaction between the junction flow and the initial condition induces a 2-contact discontinuity, which propagates forward on the outgoing link without changing the speed profile on that link.

5.3. Power consumption result

In this section we present the results of the power consumption associated with the numerical solution to the Riemann problem (18) at the junction, based on the power consumption model defined in (15).

We consider the following values for the consumption model parameters: $d = 1\,kg/m^3$, $C_D A = 0.583\,m^2$, $m = 1465\,kg$, $g = 9.8\,m/s^2$, $C_{RR} = 0.011$, $k_m = 1.1$. The numerical results for the spatial density of power consumption are illustrated in Figure 5.

For the outgoing link (solid line), one may note the increased power consumption after time $t = 3$ minutes, due to the propagation of the 2-contact discontinuity and the resulting increased flow of vehicles. In the case of link 1 (dashed line), the consumption drops suddenly with the propagation of the 1-shock wave, which causes both a decrease in flow and a decrease in speed. A similar phenomenon occurs for link 2. For all links, in this case of low speeds, the rolling drag losses are significantly larger than the aerodynamic losses.

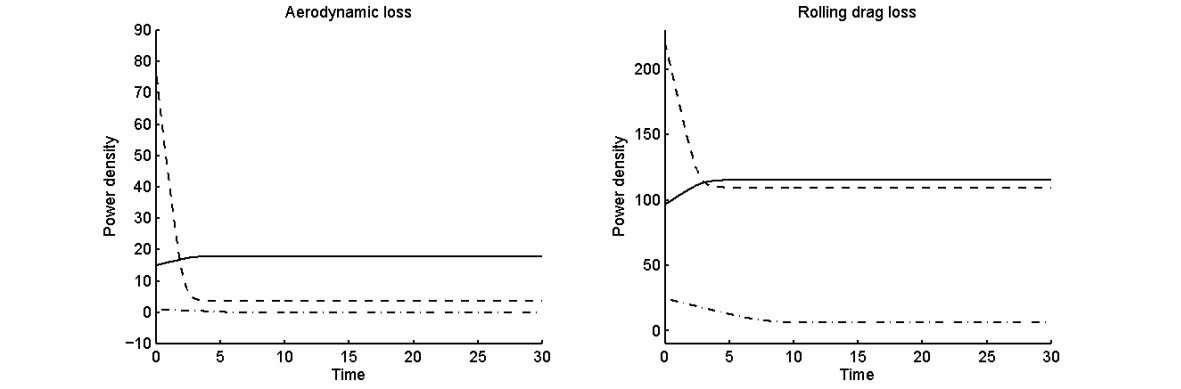

Figure 5. Average Power consumption for link 1 (dashed line), link 2 (dot-dashed line), link 3 (solid line) for the power due to aerodynamic losses (left) and rolling drag (right).

6. Conclusion

In this article we proposed a formulation for modeling network junctions in the context of the general phase transition model applied to a Greenshields flux function. The Riemann solver for the junction is constructed and a corresponding numerical scheme extending the modified Godunov scheme for the link formulation, is introduced.

Leveraging the ability of the model to propagate different types of waves (shocks and rarefactions existing in scalar models, but also contact discontinuities, phase transitions specific to this model) we numerically compute power consumption at a macroscopic level.

Extensions to this work include the construction of the Riemann solver at the junction for other flux functions applied to the phase transition model, and the consideration of bounded acceleration macroscopic models consistent with the general phase transition model in order to capture power consumption due to acceleration patterns.

References

Aw, A., Rascle, M., 2000. Resurrection of "second order" models of traffic flow. SIAM Journal on Applied Mathematics 60 (3), 916–938.

Blandin, S., Argote, J., Bayen, A., Work, D., 2011a. Phase transition model of non-stationary traffic flow: definition, properties and solution method, In review for *Transportation Research Part B*, 2011.

Blandin, S., Work, D., Goatin, P., Piccoli, B., Bayen, A., 2011b. A general phase transition model for vehicular traffic. SIAM Journal on Applied Mathematics. 71 (1), 107–121.

Chalons, C., Goatin, P., 2008. Godunov scheme and sampling technique for computing phase transitions in traffic flow modeling. Interfaces and Free Boundaries 10 (2), 195–219.

Coclite, G., Garavello, M., Piccoli, B., 2005. Traffic flow on a road network. SIAM Journal on Mathematical Analysis 36 (6), 1862–1886.

Colombo, R., 2003. Hyperbolic phase transitions in traffic flow. SIAM Journal on Applied Mathematics 63 (2), 708–721.

Colombo, R., Goatin, P., Piccoli, B., 2010. Road networks with phase transitions. Journal of Hyperbolic Differential Equations 7 (1), 85–106.

Garavello, M., Piccoli, B., 2006. Traffic flow on networks. American Institute of Mathematical Sciences, Springfield, MO.

Garavello, M., Piccoli, B., 2009. Conservation laws on complex networks. Ann. Inst. H. Poincaré Anal. Non Linéaire 26 (5), 1925–1951.

Godunov, S., 1959. A difference method for numerical calculation of discontinuous solutions of the equations of hydrodynamics. Matematicheskii Sbornik 89 (3), 271–306.

Greenshields, B., 1935. A study of traffic capacity. Proceedings of the Highway Research Board 14 (1), 448–477.

Lighthill, M., Witham, G., 1956. On kinematic waves, II: a theory of traffic flow on long crowded roads. Proceedings of the Royal Society of London 229 (1178), 317–345.

Papageorgiou, M., Blosseville, J.-M., Hadj-Salem, H., 1990. Modelling and real-time control of traffic flow on the southern part of Boulevard Peripherique in Paris: Part I: Modelling. Transportation Research Part A 24 (5), 345–359.

Richards, P., 1956. Shock waves on the highway. Operations Research 4 (1), 42–51.

Simpson, A., 2005. Parametric modeling of energy consumption in road vehicles. Ph.D. thesis, University of Queensland.

Zhang, M., 2002. A non-equilibrium traffic model devoid of gas-like behavior. Transportation Research Part B 36 (3), 275–290.